Acta Cryst. (1971). **B27**, 769

Difference Densities by Least-Squares Refinement: Fumaramic Acid

BY F. L. HIRSHFELD

Department of Chemistry, Weizmann Institute of Science, Rehovoth, Israel

(*Received* 1 *July* 1970 *and in revised form* 28 *August* 1970)

The electron-density distribution in a crystal is expressed in parametric form suitable for least-squares refinement against the X-ray intensities. The model rests on an expansion of the difference density in a basis of conveniently shaped deformation functions, both spherical and non-spherical, centred on the several atoms. The expansion coefficients are subject to refinement along with the atomic coordinates and atomic or molecular vibration parameters. As a test of the method, the difference density in fumaramic acid has been mapped by least-squares refinement, which reveals far more detail than could be obtained from the same data by conventional methods. No fully objective assessment of accuracy is available, but comparison with difference densities found in other structures by more standard procedures supports the validity of the model and its potential for extracting a maximum of information from the experimental data.

Introduction

Experimental information about electron-density distibutions in covalently bonded molecules has come mainly from X-ray diffraction studies on single crystals. These have revealed significant departures from the conventional spherical-atom model, usually in the form of residual features in difference-density maps following a spherical-atom refinement. Such a procedure has great diagnostic value but is severely deficient for quantitative mapping of actual charge distributions. Its major failing, well illustrated in a careful study by O'Connell, Rae & Maslen (1966), is the tendency of the refinement process to efface much of what the difference map is expected to reveal. The charge redistribution attendant on chemical bonding is largely absorbed in the structural parameters, especially the vibration tensors, leaving the final difference map artificially flattened. In addition, any Fourier map suffers from possible distortion by a few reflexions that may have been inaccurately measured or entirely omitted. Finally, the experimental difference map, at best, shows the difference density smeared by thermal vibration. This hampers comparison with theoretical or even with other experimental results.

Attempts to overcome the worst of these difficulties have included the use of theoretically derived non-spherical atomic form factors (*e.g.* McWeeny, 1954; Stewart, Davidson & Simpson, 1965). Studies by Cady & Larson (1965), Rae & Maslen (1965), Fritchie (1966), Verschoor (1967), and Rietveld, Maslen & Clews (1970) have introduced such form factors without, in most instances, so decisively improving the agreement between observed and calculated structure amplitudes, whether gauged by discrepancy indices or by difference maps, as to vindicate entirely the theoretical f curves.

A more flexible approach has been adopted by Dawson and others in studies on diamond and similar high-symmetry structures (Weiss, 1964; Dawson, 1965, 1967; Dawson & Sanger, 1967; Kurki-Suonio, 1968, 1969; McConnell & Sanger, 1970). The success of these studies in providing quantitative difference-density information has encouraged the hope that similar techniques can be usefully applied to structures of lower symmetry. Preliminary efforts in this direction (Mason, Phillips & Robertson, 1965; Hirshfeld & Rabinovich, 1967) concentrated on specific difference-density features, such as charge excess in the middle of a covalent bond or the contraction and polarization of bonded hydrogen atoms. More general parametric models of the charge distribution have only recently been tried (Hartman & Hirshfeld, 1969; Maslen, 1969; Willoughby & Coppens, 1969; Coppens, Csonka & Willoughby, 1970) and little experience with these has yet been reported.

Any such model seeks to represent the actual charge distribution in terms of a limited number of adjustable parameters that can be evaluated, along with the standard structural parameters, by least-squares refinement against the X-ray data. Formulation of a particular model necessarily imposes a compromise between a too restrictive *a priori* constraint and an excessive number of adjustable parameters. In seeking such a compromise we can be guided by several quite general considerations:

(*a*) Since the spherical-atom model has proven such a widely applicable approximation and is certain to be used in the initial stages of any structure analysis, it is convenient to retain this approximation as a major component of any improved model, letting the adjustable parameters describe departures from the spherical-atom charge distribution.

(*b*) Evaluation of the requisite derivatives for least-squares refinement will be simplest if the parameters are chosen as linear expansion coefficients, *i.e.* if the charge deformation is expanded in a fixed basis of density functions whose coefficients are the variable parameters.

(*c*) Appreciable charge displacements will generally be confined to the vicinity of the atoms, within distances comparable with their covalent radii, and will vary smoothly everywhere except very near the atomic centres. It is reasonable, then, to choose basis functions centred on the several atoms and falling smoothly to zero not very far from their centres. The adoption of such localized basis functions preserves the customary and very convenient partitioning of the total charge distribution into atomic fragments.

(*d*) If the basis functions are made approximately orthogonal to one another, statistical correlations among their coefficients are likely to be satisfactorily small. This is important if we wish to build up a deformation model of the requisite flexibility by successively adding new basis functions or to test the possibility of transferring deformation coefficients between similar structures. It may also be crucial to the convergence of an iterative least-squares refinement.

(*e*) A judicious choice of the shapes of the basis functions and of their spatial orientations can greatly facilitate the exploitation of symmetry arguments for minimizing the number of independent parameters to be adjusted. For example, if a molecule possesses a non-crystallographic plane of symmetry or pseudo-symmetry, it may be convenient to choose basis functions that are, singly or in pairs, symmetric with respect to this plane.

Charge-deformation model

Such considerations have led us (Hartman & Hirshfeld, 1969) to write the electron density *in a stationary molecule* as

$$\varrho = \varrho_s + \delta\varrho \,,$$

where ϱ_s is the sum of spherical free-atom densities, centred at the time-average nuclear positions. The deformation density $\delta\varrho$ is expanded as

$$\delta\varrho = \sum_l c_l \varrho_l$$

in a basis of smoothly varying functions ϱ_l, also centred on the several atoms. The scattering factor f for each atom is then computed as

$$f = f_s + \sum_l c_l \varphi_l,$$

where f_s is the spherical free-atom form factor and the sum comprises the Fourier transforms φ_l of those deformation functions ϱ_l that are centred on the particular atom. Our treatment applies to each such scattering factor the usual anisotropic temperature factor

$$t = \exp\left(-2\pi^2 h_i U^{ij} h_j\right).$$

This rectilinear harmonic approximation neglects any rotational motion of the non-spherical atom, since the vibration tensor U describes pure translation only, but this neglect should introduce no serious error if the non-spherical deformations are small and reasonably compact and the thermal vibrations are mainly translational.

For the expansion functions ϱ_l we have elected to experiment with a set of functions that are related to spherical harmonics but whose symmetry properties may be somewhat more convenient for some applications. Thus, we choose angular functions of the general form $\cos^n \theta_k$, where $n=0$, 1, 2, or 3 and the polar angle θ_k is measured from one of a specified set of $(n+1)(n+2)/2$ polar axes. The selected functions comprise one spherically symmetric function with $n=0$; three functions with $n=1$ directed along three mutually perpendicular axes $\mathbf{L}_i$; six functions with $n=2$ whose polar axes lie along the face diagonals $\mathbf{L}_i \pm \mathbf{L}_j$ of the cube built on the three axes $\mathbf{L}_i$; and ten functions with $n=3$, of which six are directed along these same face diagonals and four lie along the body diagonals. These are multiplied by the fairly arbitrarily chosen radial functions

$$R_m(r) = r^m \exp\left(-\alpha r\right),$$

where $m \geq n$ and the constant α is usually fixed so as to place the maximum of the function $R_3(r)$, on a given type of atom, at a distance $r = 3/\alpha$ that is about 1/3 to 1/2 of a typical bond length from the origin.

Table 1. *The deformation functions* $\varrho_l(\mathbf{r})$, *before orthogonalization, and their Fourier transforms* $\varphi_l(\mathbf{s})$

These are expressed in terms of the dimensionless variable $x = 2\pi s/\alpha$, where $s = 2 \sin\theta/\lambda$, and the angle ψ_k between the reciprocal radius s and the polar axis from which the angle θ_k is measured.

$\varrho_l(\mathbf{r})$	$\phi_l(\mathbf{s})$
$r_0 = \frac{\alpha^3}{8\pi} e^{-\alpha r}$	$(1+x^2)^{-2}$
$r_1 = \frac{\alpha^4}{24\pi} r e^{-\alpha r}$	$(1-x^2/3)/(1+x^2)^3$
$r_3 = \frac{\alpha^6}{480\pi} r^3 e^{-\alpha r}$	$(1-2x^2+x^4/5)/(1+x^2)^5$
$v_k = \frac{\alpha^5}{32\pi} r^2 e^{-\alpha r} \cos^2\theta_k$	$(1+x^2-6x^2\cos^2\psi_k)/(1+x^2)^4$
$\lambda_k = \frac{\alpha^4}{16\pi} r e^{-\alpha r} \cos\theta_k$	$2ix \cos\psi_k/(1+x^2)^3$
$\mu_k = \frac{\alpha^6}{64\pi} r^3 e^{-\alpha r} \cos^3\theta_k$	$3ix \cos\psi_k[3(1+x^2)-8x^2\cos^2\psi_k]/(1+x^2)^5$

The largest set of functions we have tried on a single atom comprises the following 22 products of radial and angular functions:

$$r_m = \frac{\alpha^{3+m}}{4\pi(2+m)!} R_m \ (m=0,\ 1,\ 3) \quad \text{spherically symmetric}$$

$$v_k = \frac{\alpha^5}{32\pi} R_2 \cos^2\theta_k \ (k=1,\ 2,\ \cdots 6) \quad \text{centrosymmetric}$$

$$\left.\begin{aligned} \lambda_k &= \frac{\alpha^4}{16\pi} R_1 \cos\theta_k \ (k=1,\ 2,\ 3) \\ \mu_k &= \frac{\alpha^6}{64\pi} R_3 \cos^3\theta_k (k=1,2,\cdots 10) \end{aligned}\right\} \text{anti-centrosymmetric}$$

The normalizing factors appearing here cause the integrals of the even functions r_m and v_k to equal unity. Thus the coefficients of these functions represent the net charges added to the corresponding regions, in electrons. The Fourier transforms of the listed functions are readily derived by the methods introduced by McWeeny (1951). They are presented algebraically in Table 1 and plotted in Fig. 1.

Consideration (*d*) above impels us to transform the basis functions to make them more nearly orthogonal to one another. With a suitable choice of the exponential factors α, the functions centered on different atoms will not overlap much and so will be sufficiently ortho-

Table 2. *Orthogonal basis functions derived from the* 22 *deformation functions* ϱ_l defined in Table 1

Functions λ_1, λ_2, λ_3 assumed to have their polar axes along $\mathbf{L}_1$, $\mathbf{L}_2$, $\mathbf{L}_3$, respectively. Functions v_1 to v_6 and μ_1 to μ_6 are directed successively along $\mathbf{L}_1+\mathbf{L}_2$, $\mathbf{L}_1-\mathbf{L}_2$, $\mathbf{L}_2+\mathbf{L}_3$, $\mathbf{L}_2-\mathbf{L}_3$, $\mathbf{L}_3+\mathbf{L}_1$, $\mathbf{L}_3-\mathbf{L}_1$, while $\mu_7$to μ_{10} are directed along $\mathbf{L}_1+\mathbf{L}_2+\mathbf{L}_3$, $\mathbf{L}_1-\mathbf{L}_2-\mathbf{L}_3$, $\mathbf{L}_2-\mathbf{L}_3$—$\mathbf{L}_1$, $\mathbf{L}_3-\mathbf{L}_1-\mathbf{L}_2$. Orthogonal functions v_2' to v_6', μ_2' to μ_6', and μ_8' to μ_{10}' may be derived from v_1', μ_1 , and μ_7', respectively, by appropriate sign reversals and permutation of indices. Even functions r_m' and v_k' are normalized to one electron; normalization of odd functions λ_k' and μ_k' is arbitrary.

$$\begin{aligned}
r_0' &= r_0 \\
r_1' &= -r_0 + 2r_1 \\
r_3' &= \tfrac{1}{2}r_0 - \tfrac{3}{2}r_1 + 2r_3 \\
v_1' &= -\tfrac{3}{2}r_0 + \tfrac{17}{2}r_1 + 10r_3 - 4{\cdot}910v_1 - 2{\cdot}601v_2 - 2{\cdot}122(v_3+v_4+v_5+v_6), \ etc. \\
\lambda_1' &= \lambda_1, \ etc. \\
\mu_1' &= -0{\cdot}483(\lambda_1+\lambda_2) + 1{\cdot}584\mu_1 + 0{\cdot}247(\mu_3+\mu_4+\mu_5+\mu_6) + 0{\cdot}901\ (\mu_{10}-\mu_7), \ etc. \\
\mu_7' &= -0{\cdot}235(\lambda_1+\lambda_2+\lambda_3) - 0{\cdot}901(\mu_1+\mu_3+\mu_5) + 2{\cdot}177\mu_7 - 0{\cdot}392(\mu_8+\mu_9+\mu_{10}), \ etc.
\end{aligned}$$

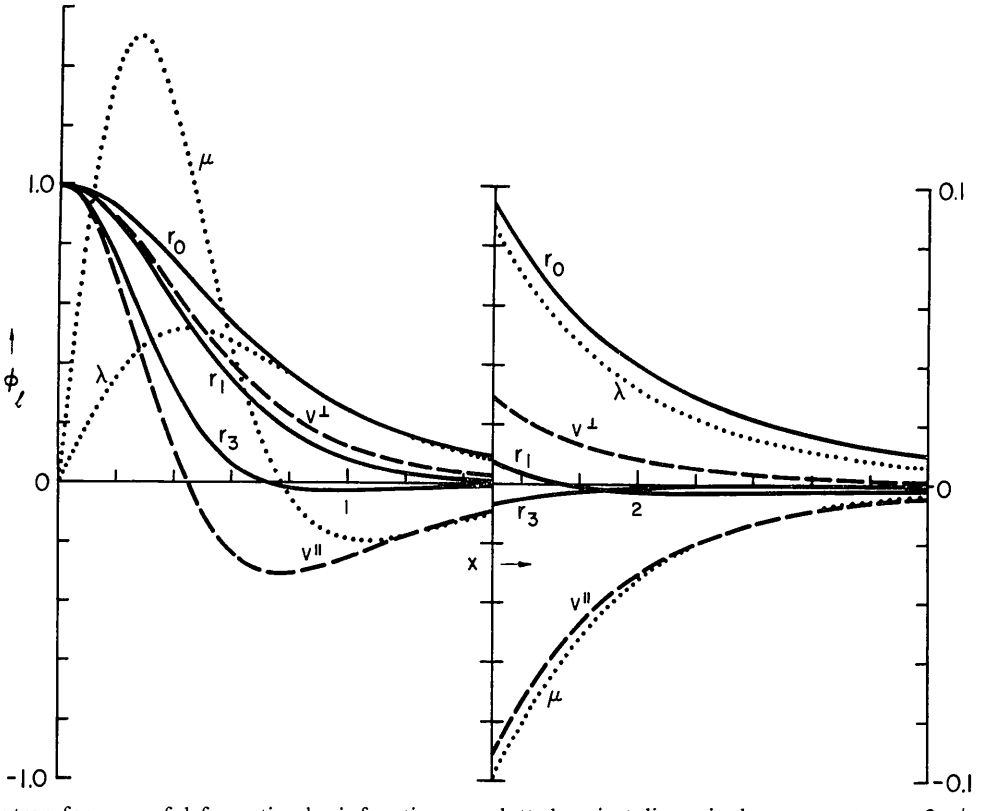

Fig. 1. Fourier transforms φ_l of deformation basis functions ϱ_l, plotted against dimensionless parameter $x=2\pi s/\alpha$. Solid curves: transforms of spherical functions r_0, r_1, and r_3; broken curves: transform of v_k in directions parallel ($v^\parallel$) and perpendicular ($v^\perp$) to polar axis; dotted curves: amplitudes of imaginary transforms of λ_k and μ_k parallel to polar axes (perpendicular components of these transforms vanish). Tenfold expansion of ordinate scale at $x=1{\cdot}5$.

gonal. On each atom, the even and the odd functions are orthogonal to one another by symmetry. What remains is to orthogonalize separately the nine even and the thirteen odd functions on each atom. This orthogonalization may be achieved, for each set, in two steps. First, a Schmidt orthogonalization is performed on the three spherical functions r_m and one of the quadratic functions v_k, in that order. By symmetry, the matrix of this transformation is the same for all six functions v_k. This matrix thus yields three new spherical functions r'_m and six new functions v'_k, the former being orthogonal to one another and to each of the latter. The six new functions v'_k are then subjected to a symmetrical orthogonalization (Löwdin, 1948). In this process they lose their axial symmetry but they retain the useful property of transforming into one another under all symmetry operations of the cube. It is primarily this property that recommends the present functions over the more familiar spherical harmonics. In analogous manner the ten cubic functions μ_k are first made orthogonal to the three linear functions λ_k and then symmetrically orthogonalized to each other. If the original 22 functions share a common value of the exponential factor α, the indicated procedure leads to the orthogonal functions listed in Table 2.

Evidently, the function space spanned by the 22 basis functions on a given centre is independent of the choice of axes $\mathbf{L}_i$. Any rotation of these axes induces a simple transformation among themselves of the three linear functions λ_k, of the six quadratic functions v_k, and of the ten cubic functions μ_k. The choice of axes is thus immaterial except for the facility that a particular choice may offer in the application of symmetry arguments. In practice, we normally define the three axes at a given atomic centre so that they are appropriately oriented with respect to supposed axes or planes of local symmetry. Such symmetry is then expressed by the vanishing of certain deformation coefficients or by the equality of sets of related coefficients. In this way the number of independently variable coefficients for a given atom may be reduced from 22 to 15 if the atom is supposed to lie in a mirror plane, 12 if on a twofold axis, 10 if at a position of symmetry *mm*, *etc.* Also, two or more identical atoms in similar environments may share identical deformation coefficients provided their coordinate axes are chosen concordantly. The application or relaxation of such constraints, as illustrated below, is one of the important ways of adapting the general deformation model to the degree of flexibility appropriate to a particular refinement.

The proposed deformation functions have admittedly been designed without regard to their compatibility with the well-established formalism of L.C.A.O. molecular-orbital theory. Unlike the atomic-orbital-product functions advocated by Stewart (1969) and employed in several recent studies (*e.g.* Maslen, 1969; Willoughby & Coppens, 1969; Coppens, Csonka & Willoughby, 1970), they do not readily lend themselves to comparisons with population analyses based on molecular-orbital wave functions. In defence of our more empirical strategy, it may be observed that neither theory nor experiment fully supports the expectation that molecular *difference* densities can be best represented *via* a minimal basis of frozen atomic orbitals. On the con-

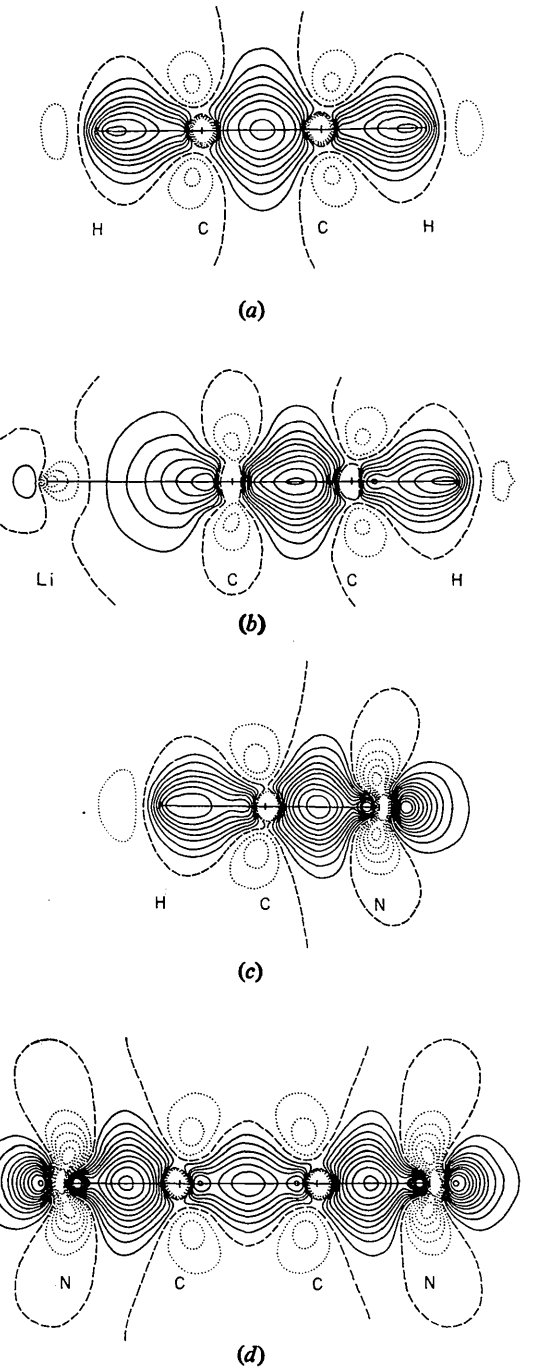

Fig. 2. Hartree–Fock difference densities (molecular electron density minus sum of spherically averaged ground-state atomic densities) computed from molecular wave functions of McLean & Yoshimine (1967). Contour interval 0·1 e.Å^{-3}, (*a*) HCCH, (*b*) LiCCH, (*c*) HCN, (*d*) NCCN.

trary, comparisons on first-row diatomic molecules (Kern & Karplus, 1964; Smith & Richardson, 1965; Ransil & Sinai, 1967) have demonstrated the sensitivity of calculated difference densities to the size, composition, and optimization of the basis sets employed. Other studies (Nesbet, 1964; Cade, Sales & Wahl, 1966; Bader, Henneker & Cade, 1967) have emphasized the importance of including polarizing functions of d and f symmetry, which are entirely absent in the atomic bases, for computations aimed at consistently interpretable molecular charge distributions. Thus it is arguable that a too dogmatic adherence to a rigid L.C.A.O. conceptual framework may hinder more than it furthers our search for an economical parameterization of experimentally observable difference densities.

Accurate theoretical studies do, on the other hand, indicate a very remarkable degree of transferability of difference densities between similar bond types in quite diverse chemical environments. Fig. 2, based on Hartree–Fock wave functions computed by McLean & Yoshimine (1967), shows that the C≡C–H portions of HCCH and LiCCH are virtually indistinguishable, as are the C≡N bond regions of HCN and NCCN. Such comparisons suggest that it may ultimately be feasible to synthesize a quite precise electron-density map of a large molecule out of fragments transferred from simpler molecules. They also appear to justify our reliance on arguments based on local symmetry and pseudosymmetry for the imposition of simplifying constraints on the deformation model.

Application to fumaramic acid

The proposed model has been tested with X-ray diffraction data from a crystal of fumaramic acid (Benghiat, Kaufman & Leiserowitz, 1971). The data were collected on a Siemens automatic diffractometer with Mo $K\alpha$ radiation through balanced filters at room temperature. They comprised a total of 1178 independent reflexions, of which 8 had net intensities smaller than half their statistical standard deviations and were treated as unobserved. Somewhat over half the measured reflexions were within the limiting sphere for Cu $K\alpha$ radiation. Beyond this sphere only reflexions with calculated structure amplitudes (after a preliminary structure refinement) above a preset level were recorded. Almost all intensity data represent averages of 2 or 4 symmetry-related reflexions, including Friedel pairs. Exhaustive comparison within equivalent sets provided an objective assessment of the experimental precision of the measured intensities and allowed the rejection of a few erroneous data.

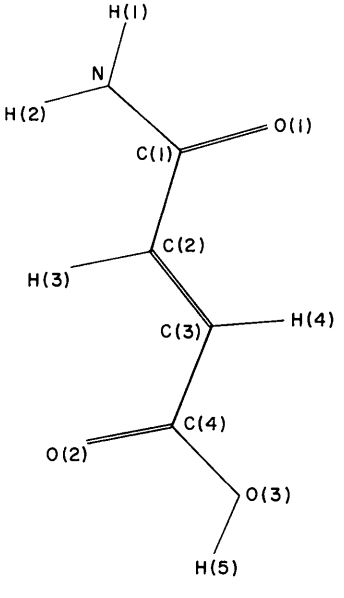

Fig. 3. Molecular formula of fumaramic acid, showing atomic numbering.

The unit cell contains two molecules in general positions related by a twofold screw axis in space group $P2_1$. Each molecule contains 13 atoms (Fig. 3). The deformation model thus permits a maximum of $13\times22=286$ independent deformation coefficients. This number was, in fact, reduced to 85 by several rather drastic approximations:

(*a*) the deformations at each atom were assumed symmetric to reflexion in a plane defined by the vectors to two neighboring atoms (approximately the mean molecular plane);

(*b*) for each of the atoms O(1), O(2), and N, a second mirror plane was assumed, perpendicular to the first and intersecting it in the appropriate C=O or C–N bond axis;

(*c*) deformation coefficients were shared between the pair of atoms C(2) and C(3), in correspondingly oriented local coordinate systems (related essentially by a local centre of symmetry midway between the two atoms), and similarly for the pair O(1) and O(2);

(*d*) identical parameters were shared by all five hydrogen atoms, which were assumed axially symmetric about their respective covalent bond axes; moreover, the eleven basis functions containing the radial dependence $R_3=r^3\exp(-\alpha r)$ were omitted for the hydrogen atoms.

With these simplifications, the independent deformation parameters consisted of

15 for C(1),
15 for C(4),
15 for the pair C(2) and C(3),
10 for the pair O(1) and O(2),
15 for O(3),
10 for N,
5 for the hydrogen atoms.

These 85 deformation coefficients were refined by an iterative least-squares routine on the Golem A computer, together with the scale factor k, 38 atomic coordinates (one y coordinate being fixed to locate the origin along the polar b axis), and 20 rigid-body molec-

ular vibration parameters; *i.e.* the atomic vibration tensors **U** were made explicitly dependent on the 20 independently variable components of the molecular vibration tensors **T**, **L**, and **S** (Schomaker & Trueblood, 1968). The spherical-atom form factors f_s for C, N, and O were taken from Berghuis, Haanappel, Potters, Loopstra, MacGillavry, and Veenendaal (1955). For hydrogen the standard ground-state f curve was used, *i.e.*

$$f^H(s)=(1+\pi^2 a_0^2 s^2)^{-2},$$

where $s=2\sin\theta/\lambda$.

The exponential factors α occurring in the radial functions were not adjustable in the least-squares refinement. However, some experimentation was performed with alternative values in an effort to establish reasonable ranges for these quantities. This experimentation consisted of several parallel refinements, which we distinguish by the labels *A*, *B*, *C*, and *D*. In most instances a single value of α was used for all functions on a given type of atom. Thus, refinement *A* had values of 4·0, 4·5, 5·0, and 5·5 Å^{-1}, respectively, for hydrogen, carbon, nitrogen, and oxygen atoms. In refinements *B* and *C* these were increased to 4·0, 5·5, 6·0, and 6·5 Å^{-1}. Refinement *D* had values of 2·0, 4·7, 5·0, and 5·3 Å^{-1} for all except the cusp functions r_0, for which the indicated values were doubled.

A standard refinement 0, with no deformation functions, was performed in the same fashion for comparison.

In examining the results of the several refinements we have four principal kinds of information to compare:

(*a*) final discrepancy indices $R=\sum||F_0-k|F_c||/\sum F_o$ and

$$r=\sum w(F_0^2-k^2|F_c|^2)^2/\sum wF_0^4;$$

(*b*) final values of the parameters and their estimated variances and covariances;

(*c*) the deformation density $\delta\varrho$ computed from the final expansion coefficients;

(*d*) the *residual* difference density $\Delta\varrho$ synthesized from the Fourier coefficients $\Delta F=(1/k)F_o-F_c$ after inclusion of the deformation functions in the evaluation of F_c.

Taken together, the results do not lead to a single best choice of deformation parameters. They do, however, help in identifying electron-density features that are fairly independent of reasonable variations in the deformation model, in estimating the range of validity of the information derivable *via* this model, and in suggesting ways of enhancing the reliability of such information.

First to be computed were refinements *A* and *B*. Of these, the discrepancy indices (Table 3) appear to favour *B*, with its larger exponential factors α. However, this refinement was suspect for several reasons. Most disturbing was the large drop in the scale factor k, compared with refinements 0 and *A*. The deformation map $\delta\varrho_B$ [Fig. 4(*b*)] showed large positive peaks at all atomic positions. Both indications made it appear that the deformation parameters were trying, not only to modify the spherical-atom density, but partly to replace it; *i.e.* that the actual scale factor k' (defined by the experimental conditions, though unknown) was larger than the least-squares value k and that the true electron density, accordingly, was approximated by $(k/k')(\varrho_s+\delta\varrho)$ with $k/k'<1$.

Some fairly sharp peaks and troughs near the atomic centres in the residual difference densities $\Delta\varrho_A$ and $\Delta\varrho_B$ suggested that significant charge-deformation features might yet remain to be incorporated properly in the model. Therefore, the exponential factors α of the r_0 functions were doubled, relative to the remaining functions, in the hope that these more sharply peaked functions might better represent the charge distribution near the atomic centres. A bit of experimentation with the exponential factors, guided by an effort to keep the scale factor near the value assigned to it by refinement 0, led to refinement *D*. This yielded discrepancy indices intermediate between those from refinements *A* and *B*. The deformation map $\delta\varrho_D$ was quite similar to $\delta\varrho_A$ except in the immediate vicinity of the atomic centres (Fig. 4). The residual difference density $\Delta\varrho_D$ was not noticeably flatter than the corresponding maps from the two pre-

Table 3. *Discrepancy indices R and r, and final values of representative parameters with their estimated standard deviations, as derived from alternative least-squares refinements*

Refinement	0	*A*	*B*	*C*	*D*
R	0·04395	0·02771	0·02645	0·02648	0·02721
r	0·00629	0·00180	0·00163	0·00163	0·00175
k	12·794 ±0·033	12·933 ±0·895	10·095 ±1·666	(12·794)	12·707 ±1·566
C(2)–H (Å)	0·946 ±0·034	1·117 ±0·046	1·023 ±0·038	1·042 ±0·040	1·121 ±0·035
C(3)–H (Å)	1·003 ±0·036	1·047 ±0·043	0·950 ±0·036	0·966 ±0·037	1·027 ±0·031
N–H(1) (Å)	0·861 ±0·027	0·983 ±0·036	0·857 ±0·034	0·871 ±0·035	0·921 ±0·031
N–H(2) (Å)	0·778 ±0·039	0·954 ±0·049	0·852 ±0·040	0·864 ±0·041	0·925 ±0·041
O–H (Å)	0·898 ±0·026	0·912 ±0·039	0·846 ±0·033	0·858 ±0·033	0·910 ±0·033
T^{11} (Å^2)	0·0227±0·0004	0·0213±0·0007	0·0198±0·0012	0·0216±0·0003	0·0210±0·0010
T^{22} (Å^2)	0·0187±0·0016	0·0206±0·0008	0·0179±0·0014	0·0197±0·0008	0·0200±0·0011
T^{33} (Å^2)	0·0252±0·0028	0·0258±0·0012	0·0242±0·0023	0·0259±0·0020	0·0252±0·0018
L_{11} (rad^2)	0·0220±0·0005	0·0200±0·0008	0·0199±0·0008	0·0199±0·0008	0·0201±0·0008
L_{22} (rad^2)	0·0006±0·0001	0·0008±0·0002	0·0007±0·0002	0·0007±0·0002	0·0007±0·0002
L_{33} (rad^2)	0·0017±0·0001	0·0016±0·0001	0·0016±0·0001	0·0016±0·0001	0·0016±0·0001
q (e)	—	−11·25	+5·76	−7·61	−40·32

vious refinements. Also, its most prominent features did not appear to conform to the assumed local symmetry. It was therefore concluded that any significant improvement in the model would require a relaxation of the symmetry constraints or some more drastic change in the nature of the basis functions rather than any modification of the numerical parameters alone.

A final experiment, refinement *C*, consisted of a repetition of refinement *B* except that the scale factor k was arbitrarily fixed at the value given by refinement 0. The discrepancy indices were scarcely increased by this constraint, as could be anticipated from the estimated standard deviation of k as derived from refinement *B*. The resulting deformation density $\delta\varrho_C$ [Figs. 4(*c*) and 5] was generally similar to $\delta\varrho_A$ and $\delta\varrho_D$.

Inspection of the discrepancy indices (Table 3) shows that the introduction of the deformation model, with no matter which set of exponential factors, has significantly improved the agreement between F_o and F_c as compared with refinement 0. The near equality of the discrepancy indices for the four refinements *A* to *D* implies that the experimental data do not permit a precise determination of the best values for the exponential factors. Comparison of the refined values of the deformation coefficients with their respective estimated standard deviations leads to a similar conclusion for these parameters; in all refinements, the final values of very few deformation coefficients differ significantly from zero. However, it is not the numerical values of the individual parameters that interest us especially but rather the deformation density $\delta\varrho$ that they collectively define. Our basis set may, in principle, be sufficiently redundant to define the deformation density quite sharply even though the individual parameters are very imprecisely determined. If so, we should expect the several deformation maps to be closely similar in appearance despite wide variations in the parameters. In part this is just what is observed.

The results show, however, that large statistical correlations occur not only among the several deformation parameters but between these and the structural parameters as well. This effect is illustrated in Table 3, which examines the interaction between the deformation model and some of the more sensitive standard parameters. The strong correlation between the deformation parameters and the scale factor, especially evident in refinement *B*, is not surprising. Its significance is considered further below. Other standard parameters expected to interact strongly with the deformation coefficients are the hydrogen coordinates and the molecular vibration parameters. Thus it is encouraging that the positions of the hydrogen atoms appear slightly more plausible when the charge deformation is explicitly included in the model than when it is excluded. This is one of the indications that the deformation model has permitted a more meaningful refinement of the structure. The effect on the vibration parameters is illustrated by the behavior of the diagonal components of the molecular translation and libration tensors **T** and **L**. These are evidently less sensitive to interactions with the deformation parameters than might have been supposed. Undoubtedly, this result is related to the presence of a large proportion of high-angle reflexions, which help to distinguish between thermal smearing of the atomic peaks and a redistribution of charge among the deformation functions of the present model. As a consequence, the estimated standard deviations of the translation components T^{ij} appear, contrary to expectation, to be often smaller in the presence of the deformation parameters than in their absence. (This comparison of standard deviations estimated from the residuals and the inverted least-squares matrix implies no ascription of objective significance to such estimates). Presumably, although no calculations were performed to test the matter, the interactions would have been far greater had individual atomic vibration tensors been refined independently or had our basis set included very much more sharply peaked cusp functions. It appears, also, that some of the larger statistical correlations between vibration and deformation parameters are mediated to an appreciable extent through their mutual interactions with the scale factor. Refinement *C*, in which the scale factor was fixed at the value derived from refinement 0, yielded values of T^{ij} near those from refinement 0 but with smaller estimated deviations. Comparisons of T^{ij} and of their standard deviations between different refinements can, however, be misleading because they refer to different molecular origins, chosen in each case to make **S** symmetric and minimize the trace of **T** (Schomaker & Trueblood, 1968).

Calculated deformation densities

Two problems arise in connexion with the explicit evaluation of the deformation density $\delta\varrho$ from the least-squares parameters. First, no constraint was applied in the refinement of the deformation coefficients to keep the net electron count constant, either for each atom or for the molecule as a whole. Consequently, if we simply summed the deformation functions with their least-squares coefficients we should obtain a deformation map with a non-vanishing integral. For example, the coefficients of refinement *D* imply a net deficit of over 40 electrons per molecule, the quantity denoted by q in the last line of Table 3. A simple way around this difficulty is to add one more basis function, with a uniform density distribution throughout space, and assign it a coefficient that restores the correct electron count for the unit cell. This device is supported by the observation that it leads consistently to near-zero values of $\delta\varrho$ at positions far from any atoms. For refinement *D* the extra term adds a uniform density of 0·33 e.Å^{-3}, not a negligible correction.

Secondly, any map obtained by direct summation would be largely dominated by the cusp densities at the atomic centres. These are just the positions where the calculated values of $\delta\varrho$ are least meaningful, both because of the large uncertainty in the scale factor and

vibration parameters and because the detailed forms of the cusp densities manifest themselves experimentally well beyond the reciprocal radii at which our data were recorded. It thus appeared preferable to moderate these peaks by a process of double Fourier inversion. 'Structure factors' were computed for a structure consisting of the deformations alone (omitting the free-atom contributions f_s to the scattering factors) with vanishing vibration parameters. These were then inserted as coefficients in a Fourier synthesis routine to

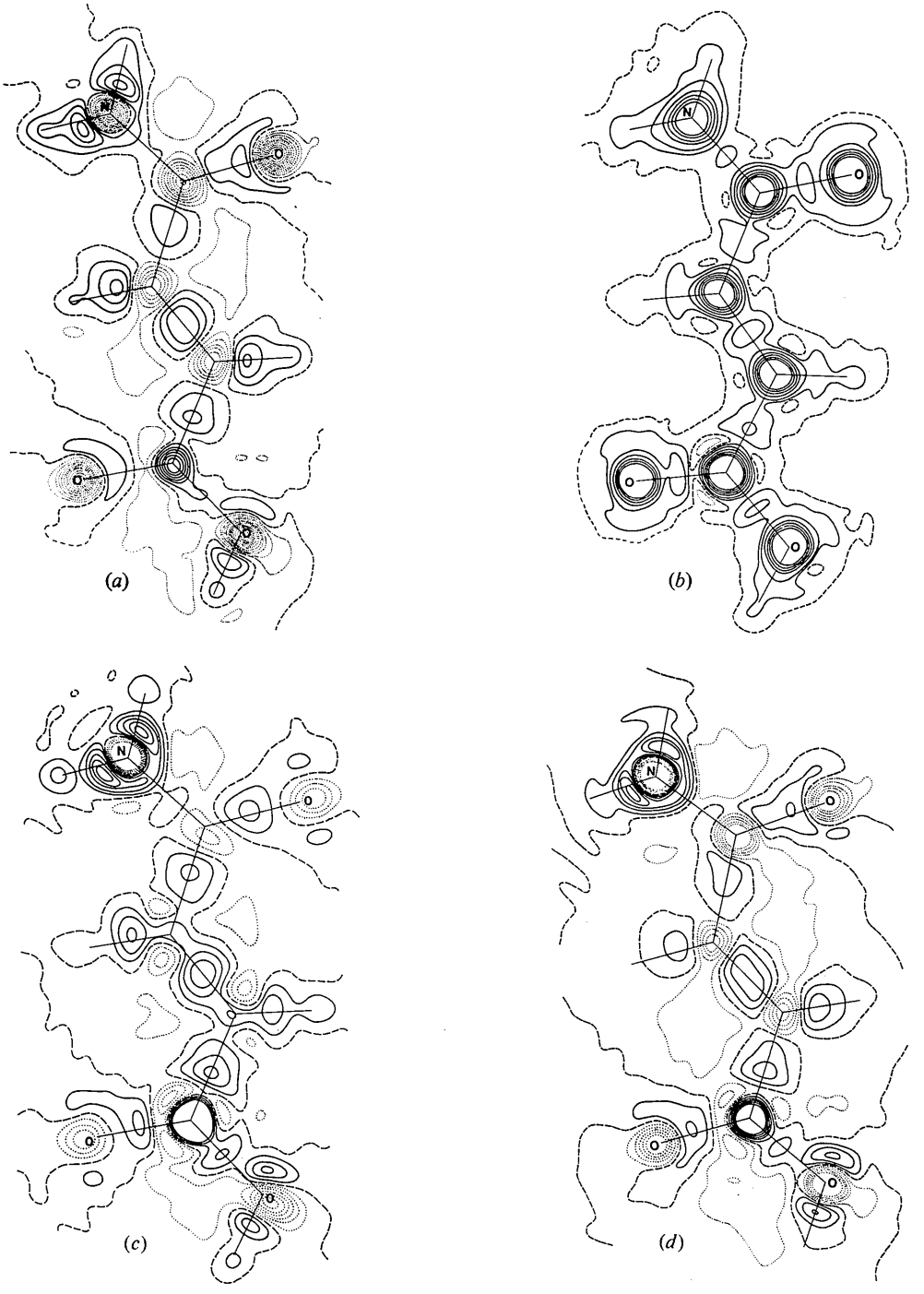

Fig. 4. Computed deformation density in mean molecular plane of fumaramic acid, derived from four least-squares refinements. (*a*) $\delta\varrho_A$: contour interval 0·2 e.Å^{-3}, (*b*) $\delta\varrho_B$: contours at −0·5, 0, 0·5, 1, 2, 3, 4, 5 e.Å^{-3}, (*c*) $\delta\varrho_C$; contour interval 0·2 e.Å^{-3}, (*d*) $\delta\varrho_D$: contour interval 0·2 e.Å^{-3}.

produce the required deformation maps (Figs. 4 and 5). For these computations a reciprocal-radius cut-off of 2·31 Å^{-1} was used, corresponding to the highest-angle reflexions recorded experimentally. Comparison between a typical $\delta\varrho$ map derived in this manner and one evaluated subsequently by direct summation from the same parameters showed that the only appreciable effects of series termination in the former map were the expected suppression of detail near the atomic centres and the introduction of spurious ripples in the zero contours.

The indirect method of computation had the incidental virtue of allowing the effect of thermal smearing to be readily simulated. Replacement of the zero vibration parameters used in the computation of $\delta\varrho$ by the appropriate rigid-body parameters obtained from the least-squares refinement led to the calculation of a vibrationally smeared deformation density $\mathbf{T}\delta\varrho$. Such a map, displaying the calculated deformation density as it would appear in a harmonically vibrating molecule, could be compared directly with the conventional difference density $\Delta\varrho_0$ from refinement 0.

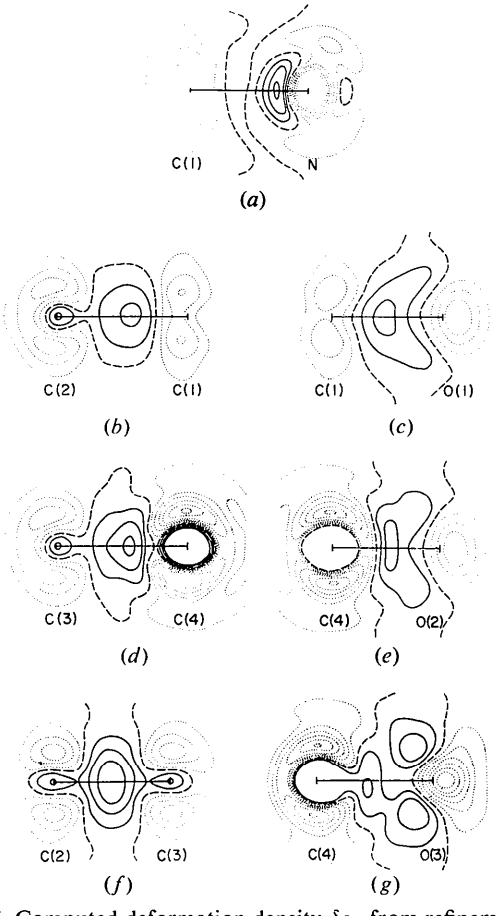

Fig. 5. Computed deformation density $\delta\varrho_C$ from refinement *C*, contour interval 0·2 e.Å^{-3}. Sections perpendicular to approximate molecular plane, containing the bonds: (*a*) C(1)–N, (*b*) C(2)–C(1), (*c*) C(1)=O(1), (*d*) C(3)–C(4), (*e*) C(4)=O(2), (*f*) C(2)=C(3), (*g*) C(4)–O(3).

Examination of the several maps shows that at most positions except within about 0·3 Å of the atomic centres the three refinements *A*, *C*, and *D* all display very much the same pattern of charge deformation. Refinement *B* is harder to interpret but it, too, shows qualitative agreement with the most prominent features of the other three. At the atomic centres, the four sets of results are so discordant, not only in magnitude but even in sign, that no significant conclusions are possible.

Features most consistently found in the several $\delta\varrho$ maps include localized peaks centred near the midpoints of the covalent bonds. Typical maxima of these peaks, as derived from refinements *A*, *C*, and *D*, are:

in the C–C single bonds	0·4 to 0·6 e.Å^{-3}
in the C=C double bond	0·6 to 0·8
in the C–OH bond	0·3
in the C=O bonds	0·4 to 0·5
in the C–N bond	0·2 or less
in the C–H and O–H bonds	0·6
in the N–H bonds	0·8 to 1·0

Most of these features occur also in $\delta\varrho_B$, with peak densities usually some two to three times higher.

The C–C and C=C bond peaks are consistently well resolved and symmetrically positioned between the bonded atoms. They are nearly spheroidal, having their greatest extension, especially in the C=C bond, normal to the molecular plane. The C–OH and C=O peaks are more diffuse; the latter extend in a bowl-shaped ridge around the oxygen atoms, ending in subsidiary maxima of about 0·25 e.Å^{-3} in the molecular plane near what may be regarded as the lone-pair regions. The C–N peak, when identifiable at all, is very diffuse. It varies in shape and position and is generally accompanied by a second much sharper peak near the nitrogen end of the bond. The peaks in the bonds to hydrogen may be sharp or broad. They often extend asymmetrically to enclose the hydrogen atoms, which may lie on secondary maxima of 0·2 to 0·4 e.Å^{-3}.

Equally interesting are the regions of charge deficiency revealed by the $\delta\varrho$ maps. Such troughs are located near the carbon atoms, on the sides opposite their bonding directions as well as along the normals to the molecular plane. They vary greatly in position, in shape, and in maximum depth, and tend to show up most prominently in refinements *B* and *C*, which had the largest values of α (in functions other than r_0). The carboxylic carbon atom, in particular, is surrounded, in $\delta\varrho_B$ and $\delta\varrho_C$, by a trigonal bipyramidal array of five troughs, some exceeding $-1{\cdot}0$ e.Å^{-3} in depth, at distances about 0·4 Å from its centre. The three other carbon atoms show similar troughs, about $-0{\cdot}7$ e.Å^{-3}, at 0·3 to 0·4 Å above and below the molecular plane (Fig. 5).

Near the oxygen and nitrogen atoms are less pronounced regions of charge depletion. This may be correlated with the relative poverty of their covalent bond peaks, compared with the bonds between carbon atoms. There are indications that the oxygen atoms

may lose charge from regions close to their centres. All $\delta\varrho$ maps show steep gradients at the oxygen positions, in the directions of the adjacent carbon atoms. Thus, in refinements *A*, *C*, and *D*, distinct troughs occur 0·05 to 0·2 Å beyond the oxygen positions, away from the carbon, while refinement *B* places the oxygen atoms on positive peaks that fall off most steeply on their far sides. In addition, all $\delta\varrho$ maps show diffuse regions of charge depletion at greater distances behind the three oxygen atoms. The apparent polarization of charge, especially near the oxygen nuclei, towards the carbon atoms to which they are linked correlates well with a consistent pattern in the C=O and C–OH bond lengths; these appear 0·006 to 0·018 Å longer in the four refinements based on the deformation model than in refinement 0.

Validity of results

Inquiry into the reliability of the computed deformation densities may usefully begin with a comparison between the results of the deformation model and those obtained by the conventional difference density method. For this purpose we can most readily compare the vibrationally smeared deformation density $\mathbf{T}\delta\varrho$ with the conventional difference density $\Delta\varrho_0$. We expect these maps to differ in two, generally opposite, ways. First, the least-squares map $\mathbf{T}\delta\varrho$ will be smoother because of the suppression of difference-density features, spurious or genuine, that do not conform to the constraints of our deformation model. On the other hand, it may show enhanced detail, compatible with this model, that was disguised in the conventional refinement by adjustments in the coordinates and vibration parameters. In comparing, for example, $\mathbf{T}\delta\varrho_D$, the vibrationally smeared deformation density from refinement *D*, with $\Delta\varrho_0$ (Fig. 6), we find clear evidence of both these effects.

Much of the fine-scale detail in $\Delta\varrho_0$, typical of background noise, is entirely absent from $\mathbf{T}\delta\varrho_D$, which has a far smoother overall appearance. At the same time, well-defined peaks and troughs occur in $\mathbf{T}\delta\varrho_D$, especially at the atomic positions and in the covalent bond regions, that are but faintly suggested, or not at all, in $\Delta\varrho_0$. It is consistent with our expectations that the most prominent of these latter features are found at the atomic centres and in the bonds to hydrogen; clearly they reflect the statistical interactions of the deformation parameters with the vibration components and the hydrogen coordinates.

We must, therefore, ask two sorts of question about the least-squares deformation densities $\delta\varrho$. How much genuine information about charge migration, perhaps dimly suggested in the erratic wiggles of $\Delta\varrho_0$ that we have dismissed as noise, has been suppressed by our arbitrary imposition on the data of a too restrictive deformation model? And how much of the charge deformation displayed in our $\delta\varrho$ maps arises simply from large statistical correlations between the standard parameters and the deformation coefficients, which permit false values of one sort of parameter at the expense of compensating errors elsewhere?

To answer the first question, we examine first the residual difference density $\Delta\varrho$ remaining after the deformation refinement. This should show any further

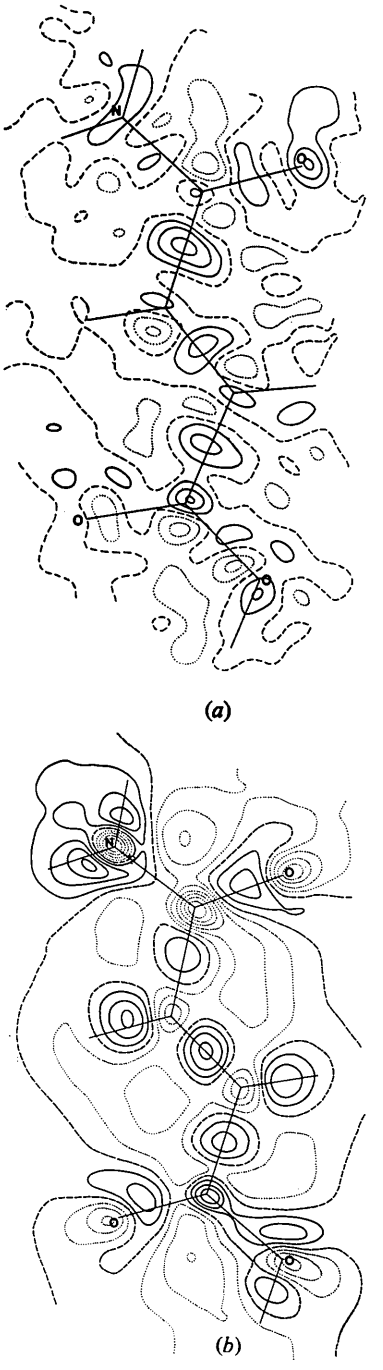

Fig. 6. Difference density in mean molecular plane of fumaramic acid as derived by conventional difference-density procedure and by least-squares refinement. Contour interval 0·1 e.Å^{-3}. (*a*) $\Delta\varrho_0$ from conventional refinement, (*b*) $\mathbf{T}\delta\varrho_D$ from refinement *D*, with vibrational smearing.

charge deformation that has failed to be accomodated by the deformation model. We can add this residual density to the vibrationally smeared deformation density $\mathbf{T}\delta\varrho$ and so obtain an augmented difference density

$$\Delta'\varrho = \mathbf{T}\delta\varrho + \Delta\varrho.$$

The Fourier coefficients of this function are just

$$\Delta'F = \frac{1}{k}F_o - F_c',$$

in which F_c' is computed from the free-atom scattering factors f_s but with structural parameters derived by use of the deformation model. In effect, we refine the structure by least squares, introducing the deformation model to overcome the systematic bias in the refinement of the standard parameters, and then compute a conventional difference map by subtracting spherical atoms at the positions and with the vibration amplitudes so derived. In this manner we avoid the greatest failing of the usual difference-density method, *i.e.* its self-effacing bias, without fully incurring the essential weakness of the deformation model, its pre-imposed constraint.

The residual difference maps $\Delta\varrho$ after refinements *A*, *B*, *C*, and *D* are all rather similar in appearance, with largest features about $\pm 0{\cdot}1$ e.Å^{-3}. The locations and shapes of these features lack any compelling chemical significance. The addition, for example, of $\Delta\varrho_D$ to $\mathbf{T}\delta\varrho_D$ makes no important difference except to reduce somewhat the magnitude and lateral extent of the two C=O bond peaks and to mask, in an apparently unsystematic fashion, the symmetry of such smaller features as the oxygen lone-pair maxima. Nothing in these maps suggests that appreciable loss of information has resulted from the use of an insufficiently flexible deformation model.

A more quantitative estimate may be derived from values of the mean square residual in F^2, measured by

$$d^2 = \sum w(F_o^2 - k^2|F_c|^2)^2/(N-p),$$

where w is the statistical weight of a reflexion

$$w = 1/\sigma^2(F_o^2),$$

N is the number of independent reflexions included in the sum, and p is the number of refined parameters. Refinement 0 yielded $d^2 = 11{\cdot}0$, whereas refinements *B* and *C* led to $d^2 = 3{\cdot}1$. Even if we suppose that our tests for internal consistency have revealed the full magnitude of the experimental errors, so that a value of $d^2 = 1{\cdot}0$ should be ultimately attainable, it is evident that most of the information about charge deformation *contained in the present data* has been uncovered by our model.

Our second question can also be given a partly quantitative answer. Any ambiguity arising out of the statistical correlations of the least-squares parameters is fully reflected in the computed variances and covariances of these parameters. True, these variances were deduced from the residuals ΔF, which contain an appreciable component of systematic error, due to the limitations of the model, in addition to their random component. By ignoring this distinction we obtain computed variances that systematically overestimate the random component of error in the final parameters. But this simply means that in applying such an estimate of the random error to judge whether or not a specially prominent feature in our $\delta\varrho$ map is genuine, we are doubly protected against the risk of too readily accepting false information. On the one hand we have overestimated the standard deviation of the computed deformation density arising from random experimental errors; on the other hand any systematic error introduced by the inflexibility of the model is more likely to have depressed the particular $\delta\varrho$ feature than to have enhanced it.

Unfortunately, application of such a conservative criterion to our $\delta\varrho$ maps affords us little comfort. For example, the estimated standard deviations of the deformation densities at the midpoints of the several carbon–carbon bonds, as derived from the covariance matrix of refinement *A* or *D*, average between 0·2 and 0·3 e.Å^{-3}. So even these bond peaks, which show up consistently in all our $\delta\varrho$ maps, appear to be less certainly established than might have been hoped. The smaller $\delta\varrho$ features we have noted, such as the oxygen lone-pair maxima or some of the less pronounced troughs around the carbon atoms, are correspondingly less certain. At the atomic centres, of course, the estimated standard deviations are so large that no meaning at all is to be attached to the erratic values of $\delta\varrho$.

If we compute standard deviations of $\delta\varrho$ from the covariance matrix of refinement *C*, however, the picture is radically different. In this refinement the scale factor k was fixed arbitrarily; hence the computed variances lack any objective significance. But they do provide a rough indication of the accuracy that might be achieved *if* we had reliable experimental measurements of the absolute intensities. What we find is that the estimated standard deviation of the deformation density $\delta\varrho_C$ is a mere 0·05 e.Å^{-3} at the middle of the C=C bond, 0·04 e.Å^{-3} at the midpoints of the two C–C single bonds, *i.e.* less than one-tenth the peak heights at these positions.

The cited results appear to be quite typical, indicating that most of the uncertainty in the computed deformation densities is directly associated with the uncertainty in the value of the scale factor. This clearly emphasizes the potential value of absolute intensity measurements. But it also means that we could, in principle, systematically vary the value assigned to k and so obtain a complete family of $\delta\varrho$ maps analogous to $\delta\varrho_C$ with the assurance that among these would be one map containing a highly accurate representation of the true deformation density.

Comparison with results of previous studies can be only qualitative because of essential differences in method. Most of the more prominent features in our $\delta\varrho$

maps have been well documented before in other structures. For example, the threefold pattern of opposed peaks and troughs surrounding a trigonal carbon or nitrogen atom has been often reported, notably in trinitro-triaminobenzene (Cady & Larson, 1965; O' Connell, Rae & Maslen, 1966), in 2,5-dimethyl-*p*-benzoquinone (Hirshfeld & Rabinovich, 1967), in cyanuric acid (Verschoor, 1964, 1967; Coppens & Vos, 1971), and in penta-*m*-phenylene and hexa-*m*-phenylene (Irngartinger, Leiserowitz & Schmidt, 1970). The symmetry of this pattern largely precludes its effacement, in conventional refinement procedures, by systematic interaction with the atomic coordinates or vibration parameters. On the other hand, the pair of troughs next to the same atoms on either side of the molecular plane can be more readily absorbed by a systematic underestimation of the out-of-plane vibration amplitudes. Thus, similarly placed troughs are seen in the accurate low-temperature study of cyanuric acid (Verschoor, 1967) but have not been reported in most of the other studies cited above. The proposed explanation conflicts, however, with the observation (Coppens, 1968) that in *s*-triazine and in deuterated α-oxalic acid dihydrate, X-ray diffraction yields consistently higher vibration amplitudes, out of plane as well as in most other directions, than does neutron diffraction. A similar difficulty confounds the interpretation of the troughs shown by our $\delta\varrho$ maps behind the oxygen atoms. Hints of correspondingly placed troughs may be found in the difference densities of 2,5-dimethyl-*p*-benzoquinone and of cyanuric acid, but in the latter structure they vanished when the atoms were located by neutron diffraction, which yielded oxygen positions *nearer* to the neighboring carbon atoms (Coppens & Vos, 1971). Similarly, no such troughs were seen in α-oxalic acid dihydrate (Coppens, Sabine, Delaplane & Ibers, 1969), whose atomic positions were determined by neutron diffraction.

Other features that appear more definitely established include the out-of-plane elongation of the peaks in the C=C and C=O bonds, supported by difference-density maps of many structures, including most of those cited above, and the positive difference density at the hydrogen positions, previously seen in 2,5-dimethyl-*p*-benzoquinone but more commonly inferred from the familiar pattern of anomalously small hydrogen vibration parameters (*e.g.* Jensen & Sundaralingam, 1964; Mason, Phillips & Robertson, 1965; Stewart, Davidson & Simpson, 1965). Lone-pair peaks near carbonyl oxygens have also been reported in other structures, most convincingly in cyanuric acid and in α-oxalic acid dihydrate.

These comparisons confirm, on the whole, both the validity of the difference-density information obtained by X-ray diffraction and the broad transferability of such information among quite dissimilar molecules. They also encourage the hope that the present deformation model can be made to yield results as reliable as the quantity and quality of the experimental data allow.

Further developments

One of the easiest ways of extending the flexibility of the deformation model is by a relaxation of some of the symmetry constraints. However, an attempt to abandon the assumption that the two carbonyl oxygen atoms are identical and conform to local *mm* symmetry (an assumption that ignores a difference of 0·04 Å between the two C=O bond lengths as well as an asymmetric disposition of hydrogen bonds) and to assign independent deformation coefficients to hydrogen atoms bonded to carbon, to nitrogen, and to oxygen made a scarcely appreciable difference in the final results. The assumption of molecular rigidity, in the face of the deviation of atom C(2) by 0·06 Å from the mean molecular plane, is highly dubious but probably necessary to prevent a catastrophic interaction between atomic vibration and deformation parameters.

More drastic modifications of the model might include the introduction of higher-order angular functions, experimentation with alternative radial dependences, *e.g.* replacing $\exp(-\alpha r)$ by $\exp(-\gamma r^2)$, and treating α, or γ, as an adjustable parameter. These changes would bring our model into line with the work of the Dawson school on diamond (Dawson, 1967; McConnell & Sanger, 1970).

Obvious experimental improvements include the measurement of absolute intensities, work at lower temperature, collection of more extensive data at large reciprocal radii, and ever greater pains to eliminate systematic as well as random errors. A most promising approach is the parallel investigation of the same structure by both X-ray and neutron diffraction (Coppens, 1967; Adrian & Feil, 1969; Duckworth, Willis & Pawley, 1969; Coppens, Sabine, Delaplane & Ibers, 1969; Willoughby & Coppens, 1969; Coppens & Vos, 1971).

Finally, the quality of the results obtained may depend critically on the judicious choice of crystal structures investigated. The proposed deformation model should succeed best with a molecule of high non-crystallographic symmetry, which assures a favourable ratio between the number of independent reflexions and the number of parameters needed for an adequate description of the charge deformation. Similarly, choice of a highly rigid molecule is important in permitting the imposition of rigid-body constraints on the vibration parameters. Also, it is clearly desirable, for the present, to concentrate on light-atom structures, in which the relative magnitude of the charge deformation we are exploring is likely to be maximal.

Financial support from the National Bureau of Standards, Washington, D.C. and from Stiftung VW is gratefully acknowledged.

References

ADRIAN, H. W. W. & FEIL, D. (1969). *Acta Cryst.* A**25**, 438.
BADER, R. F. W., HENNEKER, W. H. & CADE, P. E. (1967). *J. Chem. Phys.* **46**, 3341.

BENGHIAT, V., KAUFMAN, H. W. & LEISEROWITZ, L. (1971). To be published.
BERGHUIS, J., HAANAPPEL, IJ. M., POTTERS, M., LOOPSTRA, B. O., MACGILLAVRY, C. H. & VEENENDAAL, A. L. (1955). *Acta Cryst.* **8**, 478.
CADE, P. E., SALES, K. D. & WAHL, A. C. (1966). *J. Chem. Phys.* **44**, 1973.
CADY, H. H. & LARSON, A. C. (1965). *Acta Cryst.* **18**, 485.
COPPENS, P. (1967). *Science*, **158**, 1577.
COPPENS, P. (1968). *Acta Cryst.* B**24**, 1272.
COPPENS, P., CSONKA, L. & WILLOUGHBY, T. V. (1970). *Science*, **167**, 1126.
COPPENS, P., SABINE, T. M., DELAPLANE, R. G. & IBERS, J. A. (1969). *Acta Cryst.* B**25**, 2451.
COPPENS, P. & VOS, A. (1971). *Acta Cryst.* B**27**, 146.
DAWSON, B. (1965). *Aust. J. Chem.* **18**, 595.
DAWSON, B. (1967). *Proc. Roy. Soc.* A**298**, 264, 379, 395.
DAWSON, B. & SANGER, P. L. (1967). *Proc. Roy. Soc.* A**301**, 195.
DUCKWORTH, J. A. K., WILLIS, B. T. M. & PAWLEY, G. S. (1969). *Acta Cryst.* A**25**, 482.
FRITCHIE, C. J. JR (1966). *Acta Cryst.* **20**, 27.
HARTMAN, A. & HIRSHFELD, F. L. (1969). *Acta Cryst.* A**25**, S80.
HIRSHFELD, F. L. & RABINOVICH, D. (1967). *Acta Cryst.* **23**, 989.
IRNGARTINGER, H., LEISEROWITZ, L. & SCHMIDT, G. M. J. (1970). *J. Chem. Soc. B*, p. 497.
JENSEN, L. H. & SUNDARALINGAM, M. (1964). *Science*, **145**. 1185.
KERN, C. W. & KARPLUS, M. (1964). *J. Chem. Phys.* **40**, 1374.
KURKI-SUONIO, K. (1968). *Acta Cryst.* A**24**, 379.
KURKI-SUONIO, K. (1969). *Acta Cryst.* A**25**, S85.
LÖWDIN, P. O. (1948). *Ark. Mat. Astr. Fys.* **35**A, no. 9.
MASLEN, E. N. (1969). *Acta Cryst.* A**25**, S126.
MASON, R., PHILLIPS, D. C. & ROBERTSON, G. B. (1965). *Mol. Phys.* **9**, 277.
MCCONNELL, J. F. & SANGER, P. L. (1970). *Acta Cryst.* A**26**, 83.
MCLEAN, A. D. & YOSHIMINE, M. (1967). *Tables of Linear Molecule Wave Functions.* International Business Machines Corp., San José, California.
MCWEENY, R. (1951). *Acta Cryst.* **4**, 513.
MCWEENY, R. (1954). *Acta Cryst.* **7**, 180.
NESBET, R. K. (1964). *J. Chem. Phys.* **40**, 3619.
O'CONNELL, A. M., RAE, A. I. M. & MASLEN, E. N. (1966). *Acta Cryst.* **21**, 208.
RAE, A. I. M. & MASLEN, E. N. (1965). *Acta Cryst.* **19**, 1061.
RANSIL, B. J. & SINAI, J. J. (1967). *J. Chem. Phys.* **46**, 4050.
RIETVELD, H. M., MASLEN, E. N. & CLEWS, C. J. B. (1970). *Acta Cryst.* B**26**, 693.
SCHOMAKER, V. & TRUEBLOOD, K. N. (1968). *Acta Cryst.* B**24**, 63.
SMITH, P. R. & RICHARDSON, J. W. (1965). *J. Phys. Chem.* **69**, 3346.
STEWART, R. F. (1969). *J. Chem. Phys.* **51**, 4569.
STEWART, R. F., DAVIDSON, E. R. & SIMPSON, W. T. (1965). *J. Chem. Phys.* **42**, 3175.
VERSCHOOR, G. C. (1964). *Nature, Lond.* **202**, 1206.
VERSCHOOR, G. C. (1967). Ph. D. Thesis, Rijksuniv. te Groningen.
WEISS, R. J. (1964). *Phys. Letters*, **12**, 293.
WILLOUGHBY, T. V. & COPPENS, P. (1969). *Acta Cryst.* A**25**, S83.

Acta Cryst. (1971). B**27**, 781

The Crystal and Molecular Structure of Methylene Dithiocyanate

BY JOHN H. KONNERT AND DOYLE BRITTON

Department of Chemistry, University of Minnesota, Minneapolis, Minnesota 55455, *U.S.A.*

(*Received* 18 *November* 1969 *and in revised form* 15 *July* 1970)

Methylene dithiocyanate, $CH_2(SCN)_2$, forms monoclinic crystals in space group $I2/c$ with four molecules in a unit cell of dimensions $a=6{\cdot}667$, $b=8{\cdot}042$, $c=11{\cdot}101$ Å, $\beta=105{\cdot}25°$. The molecules are required by the space group to have symmetry 2. Three-dimensional film data were refined by least-squares methods to a conventional R index of 7·3%. The bond distances are: S–CH_2, 1·808 (6); S–CN, 1·677 (9); C–N, 1·194 (12) Å. The bond angles are: C–S–C, 98·2 (4); S–C–N, 176·4 (10); S–C–S, 115·0 (5)°. An intermolecular distance of 3·17 (1) Å between nitrogen and sulfur atoms on adjacent molecules suggests a weak intermolecular interaction. The intermolecular environments of sulfur and selenium atoms are compared in a number of compounds containing these atoms plus cyanide groups.

This investigation was motivated by a knowledge of the crystal structures of the isostructural trio: sulfur dithiocyanate (Feher & Linke, 1964), selenium dithiocyanate (Ohlberg & Vaughn, 1954), and selenium diselenocyanate (Aksnes & Foss, 1954). In all three of these compounds intermolecular distances shorter than the sum of the associated van der Waals radii were observed between nitrogen atoms and sulfur or selenium atoms. Each nitrogen atom appeared to participate in three intermolecular interactions, one with a bridging heavy atom, and the others with the heavy atoms in two different SCN or SeCN groups. The observed molecular symmetry of these molecules in the solid is *m*, *i.e.* both cyanides lie on the same side of the plane determined